

# Statistical mechanics of wormlike bundles

Claus Heussinger, Mark Bathe, and Erwin Frey  
*Arnold Sommerfeld Center for Theoretical Physics and CeNS,  
 Department of Physics, Ludwig-Maximilians-Universität München,  
 Theresienstrasse 37, D-80333 München, Germany*  
 (Dated: May 26, 2019)

We demonstrate that a semiflexible bundle of wormlike chains exhibits a state-dependent bending stiffness that alters fundamentally its scaling behavior with respect to the standard wormlike chain. We explore the equilibrium conformational and mechanical behavior of wormlike bundles in isolation, in crosslinked networks, and in solution.

PACS numbers:

In recent decades, the wormlike chain (WLC) has emerged as the standard model for the description of semiflexible polymers [1]. The defining property of a WLC is a mechanical bending stiffness,  $\kappa_f$ , that is an intrinsic material constant of the polymer. Within this framework, numerous correlation and response functions have been calculated, providing a comprehensive picture of the equilibrium and dynamical properties of WLCs [2, 3, 4]. A number of experimental studies have demonstrated the applicability of the WLC model to DNA [5] and F-actin [6], among other biological and synthetic polymers. Significant progress has also been made towards the description of the collective properties of WLCs, for example, in the form of entangled solutions. One of the hallmarks of this development is the scaling of the plateau shear modulus with concentration,  $G \sim c^{7/5}$  [7, 8, 9], which is well established experimentally [10, 11].

Another important emerging class of semiflexible polymers consists of *bundles* of WLCs [12, 13]. Semiflexible polymer bundles consisting of F-actin or microtubules are ubiquitous in biology [14], and have unique mechanical properties that may well be exploited in the design of nanomaterials [13]. Unlike standard WLCs, wormlike bundles (WLB) have a state-dependent bending stiffness,  $\kappa_B$ , that depends sensitively on the length- and time-scale on which the bundle is probed, as we noted previously [15]. In this Letter, we demonstrate that this state-dependence gives rise to fundamentally new behavior that cannot be reproduced trivially using existing relations for standard WLCs. We explore the consequences of a state-dependent bending stiffness on the statistical mechanics of isolated WLBs, as well as on the scaling behavior of their entangled solutions and crosslinked networks.

We consider in-plane bending of ordered bundles consisting of  $N = (2M)^2$  filaments of length  $L$  and bending stiffness  $\kappa_f$ . The assumption of planar bending in which twist deformations are absent allows us to consider the independent bending of  $2M$  bundle layers. Filaments are irreversibly crosslinked to their nearest neighbors by discrete crosslinks with mean axial spacing  $\delta$ . Crosslinks

are modeled to be compliant in shear along the bundle axis with finite shear stiffness  $k_\times$ , and to be inextensible transverse to the bundle axis, thus fixing the interfilament distance,  $b$ . Bundle deformations are characterized by the transverse deflection  $r_\perp(s)$  of the bundle neutral surface at axial position  $s$  along the backbone and by the stretching deformations  $u_i(s)$  of filaments  $i = -M \dots M - 1$ .

The WLB Hamiltonian consists of three contributions,  $H_{\text{WLB}} = H_{\text{bend}} + H_{\text{stretch}} + H_{\text{shear}}$ . The first term corresponds to the standard WLC Hamiltonian (in the weakly bending approximation)

$$H_{\text{bend}} = \frac{N\kappa_f}{2} \int_0^L ds \left( \frac{\partial^2 r_\perp}{\partial s^2} \right)^2, \quad (1)$$

which is the same for each of the  $N$  filaments. The second term accounts for filament stretching,

$$H_{\text{stretch}} = M k_s \delta \int_0^L ds \sum_{i=-M}^{M-1} \left( \frac{\partial u_i}{\partial s} \right)^2, \quad (2)$$

where  $k_s$  is the single filament stretching stiffness on the scale of the crosslink spacing  $\delta$ . While  $k_s$  typically corresponds to the enthalpic elasticity of a homogeneous beam, it may also represent the entropic stiffness of a WLC, for which  $k_s \equiv k_{\text{entr}} \sim \kappa_f^2/T\delta^4$ .

The third energy contribution,  $H_{\text{shear}}$ , results from the crosslink-induced coupling of neighboring filaments. To minimize the crosslink energy, any relative filament slip induced by cross-sectional rotations  $\theta = \partial_s r_\perp \equiv r'_\perp$  must be compensated by filament stretching (Fig. 1). This crosslink shear energy, which simply suppresses relative sliding motion of neighboring filaments, is given by

$$H_{\text{shear}} = \frac{M k_\times}{\delta} \int_0^L ds \sum_{i=-M+1}^{M-1} (\Delta u_i + b \frac{\partial r_\perp}{\partial s})^2, \quad (3)$$

where  $\Delta u_i = u_i - u_{i-1}$ .

For the special case of  $N = 2$ , this model reduces to the railway-track model introduced by Everaers *et. al.* in Ref. [16], where special emphasis was placed on the limit

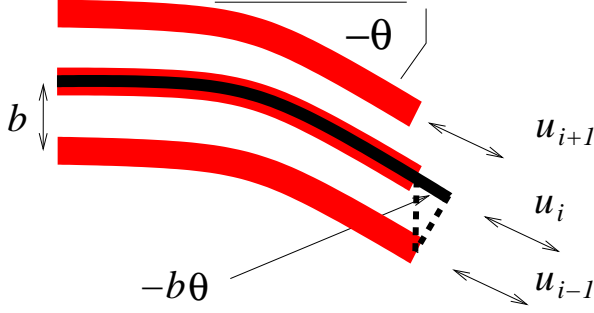


FIG. 1: Illustration of the geometry of a bundle layer. The bundle is deflected through the angle  $\theta = r'_\perp$ . If filament  $i$  stretches the amount  $u_i = u_{i-1} - b\theta$ , the crosslink (dashed line) remains undeformed with zero shear energy.

of inextensible filaments,  $k_s \rightarrow \infty$ . Here, we demonstrate that the dependence on bundle size  $N$  adds interesting and non-trivial new features to the model. By performing a similarity transformation ( $\tilde{s} = s/L$ ,  $\tilde{u} = u/b$ ,  $\tilde{r}_\perp = r_\perp/L$ ,  $\tilde{H} = HL/k_s\delta b^2$ ) one readily isolates the important coupling parameter  $\alpha = k_s L^2/k_s\delta^2$ , which describes the relative stiffness of the stretching and shearing modes. In terms of these new variables the Hamiltonian is

$$\tilde{H} = M \int_{\tilde{s}} \left[ 2M\hat{\kappa}_f \tilde{r}_\perp''^2 + \sum_{i=-M}^{M-1} \tilde{u}_i'^2 + \alpha \sum_{i=-M+1}^{M-1} (\Delta \tilde{u}_i + \tilde{r}_\perp')^2 \right]. \quad (4)$$

The dimensionless bending stiffness  $\hat{\kappa}_f = \kappa_f/k_s\delta b^2$  reduces to  $\hat{\kappa}_f = 1/12$  in the case when enthalpic filament stretching is assumed. For  $k_s = k_{\text{entr}}$  one instead finds  $\hat{\kappa}_f \sim \delta^3/l_p b^2$ , where  $l_p = \kappa_f/k_B T$  is the filament persistence length.

We are now in a position to discuss the qualitative features of the WLB model. In the limit of  $\alpha \rightarrow \infty$  the shear contribution to the bundle energy enforces  $\Delta \tilde{u}_i \equiv \Delta \tilde{u} = -\tilde{r}_\perp'$ , which implies that the stretching displacement increases linearly through the cross-section of the bundle,  $\tilde{u}_i \propto i \Delta \tilde{u}$ . This is well known from homogeneous beams [17]. Starting from this limit, decreasing  $\alpha$  reduces filament stretching at the expense of an increase in crosslink shearing. This leads to an intermediate regime in which resistance to bundle deformation is dominated by the stiffness of the crosslinks. Finally, reducing  $\alpha$  nearly to zero eliminates the crosslink shear energy, thereby rendering filaments decoupled.

Upon taking a functional derivative of the Hamiltonian the equations of motion in the free draining limit are obtained as

$$N\kappa_f r_\perp^{(4)} - \frac{2Mk_\times b}{\delta} \sum_i (\Delta u'_i + dr_\perp'') = -\zeta \frac{\partial r_\perp}{\partial t}, \quad (5)$$

$$k_s \delta u''_i + \frac{k_\times}{\delta} (\Delta u_{i+1} - \Delta u_i) = 0, \quad (6)$$

where we have assumed that the transverse deflection  $r_\perp$

is counterbalanced by the friction  $-\zeta \dot{r}$ . In this Letter we concentrate on equilibrium properties so that this term may equally be dropped. It will become important, however, in discussing dynamic quantities [18]. To proceed, Eq. (6) is solved so as to eliminate the  $u_i$  in Eqs. (4) and (5). This is equivalent to integrating out the  $u_i$  in the partition function  $Z = \int dr_\perp du_i \exp(-\beta H)$  and is analogous to the procedure presented in Ref. [19] in the context of shear-stiffened membranes. The calculations are most easily performed in Fourier-space, where we write for the expansions  $r_\perp(s) = \sum_n r_n \sin(n\pi s/L)$  and  $u_i(s) = \sum_n u_{in} \cos(n\pi s/L)$ , applicable to pinned boundary conditions [25]. The resulting equation of motion for  $r_n$  then takes the simple form

$$\kappa_n q_n^4 r_n + \zeta \dot{r}_n = F_n, \quad (7)$$

with a wave-number dependent effective bending stiffness  $\kappa_n$ . Here, an external force  $F(s) = \sum_n F_n \sin(n\pi s/L)$  has been added, which could be a random thermal force or, for example, a static tip load. The general result for  $\kappa_n$  is obtained using the standard ansatz  $u_i \sim w^i$ , which reduces Eq. (6) to an equation that is quadratic in  $w$ .

In the following, we present an approximate solution to Eq. (6) that is based on the assumption that filament stretching increases *linearly* through the bundle cross-section,  $u_i = \Delta u \cdot (i+1/2)$ , as in the limit  $\alpha \rightarrow \infty$  [24]. Although comparison with the exact solution demonstrates that  $u_i$  in general varies nonlinearly with  $i$ , it turns out that the effective bending stiffness  $\kappa_n$  is insensitive to this nonlinearity. At the same time, the linearization simplifies the formulas substantially, so that the effective bending stiffness is given in closed form by

$$\kappa_n = N\kappa_f \left[ 1 + \left( \frac{12\hat{\kappa}_f}{N-1} + (q_n \lambda)^2 \right)^{-1} \right], \quad (8)$$

where we have defined the length-scale  $\lambda = (L/\sqrt{\alpha(L)})\sqrt{\hat{\kappa}_f M/(M-1/2)}$ , which depends on the specific properties of the given bundle but not on its length,  $L$ .

For any given wavenumber  $q_n \sim n/L$ , three different elastic regimes emerge as asymptotic solutions for  $N \gg 1$  and respective values of  $\alpha$  [15]. *Decoupled bending* of  $N$  laterally independent, but transversely constrained, filaments is found in the limit of  $\alpha \rightarrow 0$ , where the bending stiffness is simply  $\kappa_n = N\kappa_f$ . In the opposite limit of  $\alpha \rightarrow \infty$  the *fully coupled* bending scenario is obtained, where the bundle behaves like a homogeneous beam with  $\kappa_n \sim N^2 k_s$  ( $\alpha \gg N$ ). Finally, the bending stiffness in the intermediate or *shear dominated* regime ( $1 \ll \alpha \ll N$ ) is  $\kappa_n \sim N k_\times q_n^{-2}$  and the full mode-number dependence has to be accounted for. It is worthwhile to note that in the continuum limit (fixing the bundle aspect ratio) Eq. (8) reduces to the well-known Timoshenko model for beam bending, which was recently used to interpret bending

stiffness measurements on grafted microtubules [20] and carbon nanotube bundles [13].

For fixed values of  $(N, \alpha)$ , the bundle bending stiffness crosses over from fully coupled to decoupled bending via the intermediate regime as the wavenumber  $q_n$  is increased. Thus, different modes may belong to different elastic regimes, rendering the fluctuation properties of the bundle non-trivial and qualitatively different from single semiflexible polymers. This cross-over is mediated by the length-scale  $\lambda$ , which acts as a cut-off on the fluctuation spectrum: whereas wavelengths  $q_n^{-1} \ll \lambda$  belonging to the decoupled regime are characterized by a constant bending stiffness, modes with  $q_n^{-1} \gg \lambda$  acquire a higher stiffness  $\kappa_n \sim q_n^{-2}$  and are thereby suppressed. Finally, for even longer wavelengths  $q_n^{-1} \gg \lambda\sqrt{N}$ , the bending stiffness reattains a constant, limiting value.

In situations where modes pertaining to the intermediate regime are irrelevant, the  $q$ -dependence of  $\kappa_n$  drops out and one recovers the single WLC result, albeit with a renormalized persistence length  $l_p \rightarrow Nl_p$  in the decoupled, and  $l_p \rightarrow N^2l_p$  in the fully coupled, regimes, respectively. In other cases, calculation of the tangent-tangent correlation function demonstrates that the persistence length cannot be defined unambiguously. As indicated in Ref. [16], the correlation function does not decay exponentially, but rather exhibits a complex structure at intermediate distances [18]. In the following, we will therefore explore the consequences on the statistical mechanics of the WLB in particular as regards the intermediate regime.

First, consider the force-extension relation as calculated from the end-to-end distance  $R(F) = L - \sum_n k_B T / (\kappa_n q_n^2 + F)$ , where  $F$  is the force applied to the bundle ends [26]. For small stretching forces one may readily calculate the linear response coefficient  $k_{\text{entr}} = F / (R(F) - R(0))$  using a Taylor series expansion. The result in the intermediate regime is

$$k_{\text{entr}} \propto \frac{(N\kappa_f)^2}{L\lambda^3 k_B T}, \quad (9)$$

which is inversely proportional to bundle length, like a mechanical beam. Importantly, the strong dependence of  $k_{\text{entr}}(L) \sim L^{-4}$  applicable to single filaments (and the other two regimes) is lost. This has dramatic consequences on the plateau value of the shear modulus  $G$  in crosslinked bundle networks, which in affine theories [21] is assumed to be given in terms of  $k_{\text{entr}}$  by  $G \sim k_{\text{entr}}(\xi)/\xi$ , where the mesh-size  $\xi$  depends on concentration  $c$  as  $\xi \sim c^{-1/2}$ . Accordingly, in the intermediate regime one finds  $G \sim c$ , which is a much weaker concentration-dependence than  $G \sim c^{5/2}$  [22] applicable to single filaments. It is worthwhile noting that the force-extension relation is strongly nonlinear (see Fig. 2), rendering the linear approximation valid only for very small relative extensions. In this particular example the linearized formula deviates from the exact solution by 50%

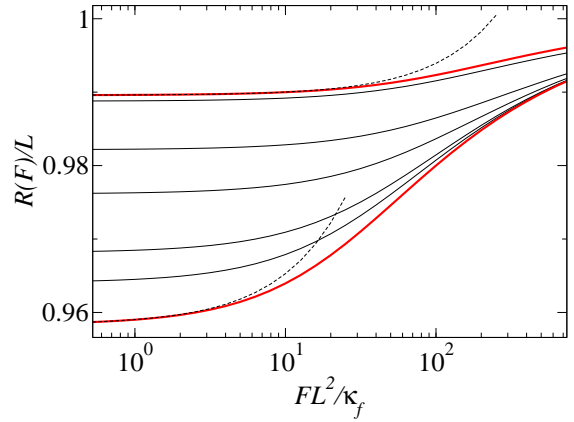


FIG. 2: End-to-end distance  $R(F)/L$  as a function of stretching force  $FL^2/\kappa_f$  for a bundle of  $N = 4$  filaments and  $L = l_p$ . The black curves correspond to  $\lambda/L = 0.01, 0.1, \dots, 0.7$ . Thick red curves relate to (bottom) decoupled and (top) fully coupled bending, respectively. Dashed lines correspond to the respective linear response regimes.

at only  $\approx 3\%$  and  $\approx 0.7\%$  in the decoupled and the fully coupled limits, respectively.

Bundle behaviour under compressive forces further highlights the unusual properties of WLBs. Because the bending stiffness in the intermediate regime scales with the length of the bundle as  $\kappa_B \sim L^2$ , the Euler buckling force  $F_c \sim \kappa_B/L^2 \sim N\kappa_f/\lambda^2$  is *independent* of bundle length. This unique property may well be exploited in polymerizing biological bundles such as filopodia, which may increase their contour length against compressive loads without loss of mechanical stability.

Complementary to the elasticity of crosslinked networks of WLBs, we turn next to the elasticity of their entangled solutions. The generally accepted theory for the concentration dependence of the plateau modulus of entangled WLCs is based on the free energy change  $\Delta F$  of confining a polymer to a tube of diameter  $d$  [7, 8]. The associated change in free energy is written as  $\Delta F \sim k_B T L / l_d$ , which defines the deflection length  $l_d$  to be the scale at which the polymer starts to interact with its enclosing tube. The deflection length itself is connected to the tube diameter  $d$  and the filament concentration  $c$  via the standard excluded volume argument [9],  $l_d^2 d = l_d / c L$ , which balances the excluded volume of the tube with the available volume per filament. All that remains is the calculation of the tube diameter  $d$  of a single polymer confined by the potential

$$V = \frac{N\kappa_f}{2l_c^4} \int_0^L ds r_\perp^2(s), \quad (10)$$

where the confinement length  $l_c$  is defined as a measure of the strength of the potential. While  $l_c \equiv l_d$  in the standard WLC, we will see shortly that this does not hold for WLBs in the intermediate regime. First, consider

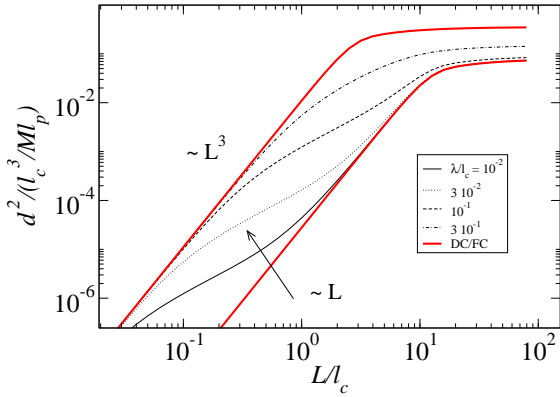


FIG. 3: Tube diameter  $d^2/(l_c^3/Nl_p)$  as a function of contour length  $L/l_c$  for various  $\lambda/l_c$  and  $M = 20$ . Thick (red) curves correspond to (top) decoupled and (bottom) fully coupled bending, respectively. For short filaments the intermediate regime is visible through the linear slope  $d^2 \sim L$  (see Eq. (11)). For long filaments the fluctuations saturate. By increasing  $\lambda$  the plateau is enhanced and the tube is becoming wider (Eq. (12)).

the transverse fluctuations of an unconfined bundle, in particular the average value  $d_0^2 \equiv \frac{1}{L} \int_s \langle r_\perp(s)^2 \rangle$ . This is most easily calculated as

$$d_0^2 \sim L\lambda^2/Nl_p, \quad (\lambda\sqrt{N} \gg L \gg \lambda) \quad (11)$$

which has to be compared to the WLC result for which  $d_0^2 \sim L^3/l_p$ . In the presence of the confining potential, the same calculation yields

$$d^2 \sim l_c^2\lambda/Nl_p, \quad (\lambda\sqrt{N} \gg l_c \gg \lambda). \quad (12)$$

For strong confinement  $l_c \ll \lambda$ , the potential suppresses all modes for which the bending stiffness belongs to the intermediate regime and one recovers the expression valid for single filaments,  $d^2 \sim l_c^3/l_p$ . The general result for the tube diameter is depicted in Fig. 3. As the contour length  $L$  of the bundle is increased it begins to “feel” the presence of its enclosing tube at the deflection length  $L = l_d$ . By comparing Eq. (11) with Eq. (12) one finds  $l_d \sim l_c^2/\lambda$ , which is valid in the intermediate regime. At the same time,  $l_d \equiv l_c$  in the decoupled and fully coupled regimes, where the deflection and confinement lengths are identical.

One may use these results to rewrite the deflection length as a function of concentration  $c$ . In the intermediate regime (weak confinement) the result is  $l_d^3 \sim Nl_p/(\lambda c L)^2$ , which replaces the usual result  $l_d^5 \sim Nl_p/(c L)^2$  valid in the decoupled regime (strong confinement). The free energy of confinement and the elastic plateau modulus  $G \sim (c L) \Delta F/L$  now depend on  $\lambda$  and thus on the properties and density of the crosslinks. The modulus displays a cross-over that is *mediated by concen-*

*tration*,

$$\beta G \sim \begin{cases} (c L)^{5/3} (Nl_p)^{-1/3} \lambda^{2/3}, & c \ll c^*, \\ (c L)^{7/5} (Nl_p)^{-1/5}, & c \gg c^*, \end{cases} \quad (13)$$

where we defined the cross-over concentration as  $(c L)^* \sim \sqrt{Nl_p} \lambda^{-5/2}$ . Below the even smaller concentration  $c^{**} \sim c^* N^{-3/4}$ , the fully coupled regime is entered and the modulus again scales as  $G \sim c^{7/5}$ .

Having discussed equilibrium properties of WLBS, further consequences of the state-dependent bending stiffness on dynamic response functions remain to be explored, along with the effects of nonpermanent crosslinks. Additional experiments [12, 13, 23, 24] are required to test the applicability of the presented results to biological and synthetic bundles.

---

- [1] N. Saitô, K. Takahashi, and Y. Yunoki, *J. Phys. Soc. J. **22***, 219 (1967).
- [2] R. Granek, *J. Physique II **7***, 1761 (1997).
- [3] J. F. Marko and E. D. Siggia, *Macromolecules **28***, 8759 (1995).
- [4] J. Wilhelm and E. Frey, *Phys. Rev. Lett. **77***, 2581 (1996).
- [5] C. Bustamante, J. F. Marko, E. D. Siggia, and S. Smith, *Science **265***, 1599 (1994).
- [6] L. L. Goff, O. Hallatschek, E. Frey, and F. Amblard, *Phys. Rev. Lett. **89***, 258101 (2002).
- [7] H. Isambert and A. C. Maggs, *Macromolecules **29***, 1036 (1996).
- [8] T. Odjik, *Macromolecules **16***, 1340 (1983).
- [9] A. N. Semenov, *J. Chem. Soc. Faraday Trans. **86***, 317 (1986).
- [10] B. Hinner, *et. al.*, *Phys. Rev. Lett. **81***, 2614 (1998).
- [11] J. Xu, A. Palmer, and D. Wirtz, *Macromolecules **31***, 6486 (1998).
- [12] M. M. A. E. Claessens, M. Bathe, E. Frey, and A. R. Bausch, *Nature Mat. **5***, 748 (2006).
- [13] A. Kis, *et. al.*, *Nature Mat. **3***, 153 (2004).
- [14] H. Lodish, *et. al.*, *Molecular Cell Biology*, 5th ed. (Palgrave Macmillan, 2003).
- [15] M. Bathe, C. Heussinger, M. Claessens, A. Bausch, and E. Frey, *q-bio.BM/0607040*, 2006.
- [16] R. Everaers, R. Bundschuh, and K. Kremer, *Europhys. Lett. **29***, 263 (1995).
- [17] L. D. Landau and E. M. Lifshitz, *Theory of Elasticity*, 3rd ed. (Butterworth-Heinemann, Oxford, 1995), Vol. 7.
- [18] C. Heussinger *et. al.*, in preparation.
- [19] D. Nelson and L. Peliti, *J. Physique **48***, 1085 (1987).
- [20] F. Pampaloni, *et. al.*, *PNAS **103***, 10248 (2006).
- [21] M. Rubinstein and R. H. Colby, *Polymer Physics* (Oxford University Press, New York, 2003).
- [22] F. C. MacKintosh, J. Käs, and P. A. Janmey, *Phys. Rev. Lett. **75***, 4425 (1995).
- [23] O. Lieleg *et. al.*, *cond-mat/0611752*.
- [24] J. A. Tolomeo and M. C. Holley, *Biophys. J. **73***, 2241 (1997).
- [25] The calculation can also be performed for more general boundary conditions, where the eigenfunctions of the bi-harmonic operator must be used.

[26] Note, that a second contribution from the finite extensibility of the bundle backbone is neglected here, for simplicity.